Reentrant Phase Diagram of Network Fluids

J. Russo,[1] J. M. Tavares,[2,3] P. I. C. Teixeira,[2,3] M. M. Telo da Gama,[3,4] and F. Sciortino[5]

[1]*Dipartimento di Fisica, Università di Roma La Sapienza, Piazzale Aldo Moro 2, 00185 Roma, Italy*
[2]*Instituto Superior de Engenharia de Lisboa, Rua Conselheiro Emídio Navarro 1, P-1950-062 Lisbon, Portugal*
[3]*Centro de Física Teórica e Computacional, Avenida Professor Gama Pinto 2, P-1649-003 Lisbon, Portugal*
[4]*Departamento de Física, Faculdade de Ciências da Universidade de Lisboa, P-1749-016 Lisbon, Portugal*
[5]*Dipartimento di Fisica and CNR-ISC, Università di Roma La Sapienza, Piazzale Aldo Moro 2, 00185 Roma, Italy*
(Received 2 September 2010; revised manuscript received 28 November 2010; published 25 February 2011)

We introduce a microscopic model for particles with dissimilar patches which displays an unconventional ''pinched'' phase diagram, similar to the one predicted by Tlusty and Safran in the context of dipolar fluids [Science **290**, 1328 (2000)]. The model—based on two types of patch interactions, which account, respectively, for chaining and branching of the self-assembled networks—is studied both numerically via Monte Carlo simulations and theoretically via first-order perturbation theory. The dense phase is rich in junctions, while the less-dense phase is rich in chain ends. The model provides a reference system for a deep understanding of the competition between condensation and self-assembly into equilibrium-polymer chains.

DOI: 10.1103/PhysRevLett.106.085703 PACS numbers: 64.60.aq, 47.57.J−, 64.70.Nd, 75.50.Mm

Almost a decade ago, Tlusty and Safran (TS) [1] predicted a topological phase separation in dipolar fluids which differs from the standard liquid-vapor phase transition of isotropically aggregating particles. Indeed, in dipolar fluids, the strong anisotropic interaction favors a nose-to-tail alignment of the dipoles and the formation on cooling of long equilibrium-polymer chains, generating a competition between self-assembly and condensation which appears to suppress the standard gas-liquid phase separation [2–7]. The TS mean-field theory assumes that stable chains are formed and focuses on the thermally excited defects of the infinite chain ground state rather than on the monomers themselves. These topological defects are identified as chain ends and junctions; their concentration is temperature T and density ρ dependent. Under specific choices of the energy cost of forming a defect, a first-order phase transition is expected to take place at low T and ρ, arising from the competition between a low-density phase rich in chain ends, and a high-density phase rich in junctions. The theory predicts an unusually low critical T and ρ behavior, and its distinctive feature is a ''pinched'' phase diagram, i.e., a coexistence region in which the coexistence ρ of the dense phase decreases and approaches the ρ of the less-dense phase, both vanishing as the T is decreased. Interestingly, the specular case, in which the gas density approaches the liquid density on cooling, has been recently reported [8].

Besides magnetic fluids, the TS theory was shown [9] to have physical implications for broad classes of systems such as gels, microemulsions and wormlike micelles. It is thus of utmost importance to design a simple (and amenable to analytic studies) microscopic model in which it is possible to tune the energy scales for chaining and for branching and which offers us the possibility to validate the topological phase transition proposed by TS and to shed light on the competition between chaining and branching. One of the most promising routes to address the problem is the study of patchy particles, which not only can model angular-dependent, limited valence interactions [10], but can also be designed, via dissimilar patches [11,12], to independently control chaining and branching. Indeed, theoretical investigations [11,12] based on the parameter-free Wertheim thermodynamic perturbation theory [13,14] suggest that, under specific choices of the energy scale of the interactions, the free energy of particles with dissimilar patches can be related to the TS expression, providing a liquid-state based alternative interpretation of the TS theory.

In this Letter we introduce a microscopic patchy-particle model specifically designed to incorporate the physics of chaining and branching [11,12,15] and which can be accurately studied numerically as well as theoretically. The model consists of hard-sphere particles of diameter σ (hereby taken as the unit of length), whose surface is decorated by patches of two different types, A and B. Two patches of type A are placed on the poles and account for the aggregation of particles in linear chains, f patches of type B are equally spaced along the equator. Different particles interact via AA bonds (with an energy scale ϵ_{AA}) or via AB bonds (with an energy scale ϵ_{AB}). The interaction between patches is described by the Kern-Frenkel potential [16,17]. In the following, T is measured in units of ϵ_{AA}/k_B (where k_B is the Boltzmann constant and $\beta \equiv 1/k_B T$) and number density in units of σ^{-3}. In this model, the number of junctions n_j (in the TS language) is equivalent to the number of AB bonds present in the system. Similarly, the number of ends n_e is provided by the number of patches of type A which are not bonded. A schematic representation

 © 2011 American Physical Society

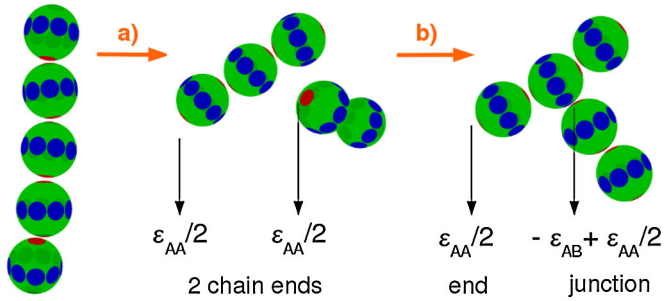

FIG. 1 (color online). Schematic representation of the patchy-particle model (two A sites are placed on the poles and nine B sites are placed along the equator), and of the energy cost of forming topological defects. Starting from a linear chain configuration (top), the figure displays the steps involved in the formation of (a) two ends, and (b) one end and one junction. From this, one can evaluate, in the TS language, the cost of creating an end as $\epsilon_e \equiv \epsilon_{AA}/2$ and the cost of forming a junction as $\epsilon_j \equiv -\epsilon_{AB} + \epsilon_{AA}/2$. In the online-color version the A and B sites are colored in red and blue, respectively.

of the model can be seen in Fig. 1. The same figure schematically explains also the mapping between the bond energy scale of the present model and the energy scale of the topological defects introduced by TS. The energy cost ϵ_{AA} of breaking a chain is twice the energy cost of a chain end (since a break produces two chain ends), while forming a junction costs $\epsilon_j \equiv \epsilon_{AA}/2 - \epsilon_{AB}$.

The emergence of pinching is a consequence of the change in the ground state of the system when ϵ_j changes sign. In the usual liquid vapor coexistence (as obtained in [15] for the present model with $\epsilon_j < 0$), as T decreases, the low density (vapor) phase approaches an ideal gas, and the high density (liquid) approaches the disordered ground state. As a result, the differences in internal energy (ΔU), entropy (ΔS), and volume (ΔV) between the vapor and the liquid phases increase when T decreases. In the present model, for $\epsilon_{AB} < \epsilon_{AA}/2$ or $\epsilon_j > 0$, the ground state is composed of unbranched structures (infinite AA chains or rings). Since there is no phase separation between an ideal gas and a fluid of chains (e.g., [10]), the coexisting phases arise from an interplay of the thermal excitations (or defects) of the ground state fluid of chains: a low ρ, high energy phase rich in ends, and a high ρ, low energy phase rich in junctions. As T is lowered, the number of defects decreases, both phases approach the ground state, and thus ΔU, ΔS, and $\Delta V \to 0$. In this Letter, we investigate the case of $\epsilon_{AB} = 0.37\epsilon_{AA}$. To favor the formation of a sufficiently large number of junctions we have placed $f = 9$ B patches, equally spaced over the particle equator.

The structural and thermodynamic properties of the model are calculated by solving the first-order perturbation theory of Wertheim and by numerical simulations. Wertheim's theory was developed in the context of associating liquids and has proven a very powerful framework for parameter-free calculations of the thermodynamic properties of patchy models [10,18,19]. According to the theory, the free energy can be written as a sum of the reference hard-sphere free energy and a bonding contribution

$$\frac{\beta F_b}{N} = 2\log X_A + f\log X_B - X_A - \frac{f}{2}X_B + \frac{1}{2}(2+f), \tag{1}$$

where X_A and X_B are, respectively, the fraction of sites A and B which are not engaged in a bond. X_A and X_B can be calculated through the law of mass action [12]

$$\begin{aligned} X_A + 2\phi\Delta_{AA}X_A^2 + f\phi\Delta_{AB}X_AX_B &= 1, \\ X_B + 2\phi\Delta_{AB}X_AX_B &= 1, \end{aligned} \tag{2}$$

where $\phi = Nv_s/V$ is the volume fraction, v_s is the volume of the sphere of diameter σ, and the quantities $\Delta_{\alpha\beta}$ ($\alpha, \beta = A, B$) are given by $\Delta_{\alpha\beta} = 1/v_s \int g_{\rm HS}(\mathbf{r})[\exp(\beta\epsilon_{\alpha\beta}) - 1]d\mathbf{r}$, where the integral involving the hard-sphere radial distribution function $g_{\rm HS}(\mathbf{r})$ [20] extends over the volume of bonding [17].

To determine the phase behavior numerically we run successive umbrella sampling Monte Carlo (MC) simulations [21], which allows us to evaluate the full density probability distribution $P(\rho)$ at fixed chemical potential μ and T. This method partitions the density region to be explored in windows of ΔN particles. Each region is sampled with grand-canonical simulations, with appropriate boundary conditions [22], allowing for effective parallelization. Sampling is very difficult specially at low T, where the pinched phase separation is predicted to occur. Indeed, at the lowest studied T, the probability of breaking a AA bond becomes of the order of $\exp(1/0.045)$, thus requiring $\sim 4 \times 10^9$ MC attempts for successfully breaking such bond. Any unbiased algorithm that generates trial positions and orientations at random will therefore be highly ineffective, either missing the formation of bonded configurations, or getting trapped once a bonded configuration is found. To overcome this problem we adapted the aggregation-volume-bias MC algorithm [23] (AVBMC). We first define the regions in space where bonding occurs and then, for each randomly selected particle, we either move a particle out of the bonding volume, or bring a particle in the bonding volume, accepting the move with the proper acceptance probability [23]. A MC step comprises GC insertion or removal moves, AVBMC moves, and ordinary Metropolis translational and rotational moves (the frequency of the three moves is, respectively, 1:500:500). At the two lowest investigated T, the length of the chains of AA particles becomes comparable to the simulation box size. To avoid spurious size effects, we have rejected moves generating AA chains of infinite length via periodic boundary conditions. Through a finite-size analysis, we have checked that these configurations have vanishing probability as the box side is increased. To evaluate the coexistence μ and the corresponding $P(\rho)$, implementing the equal area rule,

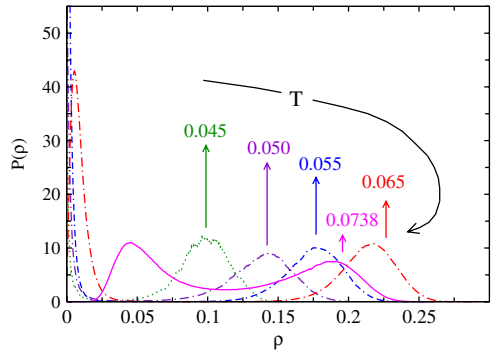

FIG. 2 (color online). Density histogram at coexistence for several T values. The average ρ of the less-dense phase is monotonically decreasing on cooling, while the average ρ of the dense phase has a nonmonotonic behavior with T. The histogram at the critical point ($T = 0.0738$) is depicted as a continuous line.

we used histogram reweighting techniques [24]. The critical point is determined from both the energy and ρ histograms of a nearby point, and then reweighting the distributions to obtain the best possible fit to the universal Ising distribution [25]. The calculated $P(\rho)$ at several different T (these data have required in total more than 10 years of CPU time) are shown in Fig. 2, while information on the coexistence μ and system sizes are reported in Table I. Interestingly, the position of the high-density peak has an unconventional reentrant behavior when lowering T, starting to decrease below $T = 0.065$. To our knowledge, this is the first time that a pinched phase diagram is directly observed.

The average densities of the two peaks of $P(\rho)$ provide precise estimates of the two coexisting densities. It is then possible to evaluate from data in Fig. 2 the full phase diagram of the model, down to $T = 0.045$. The res ults are shown as symbols in Fig. 3, where the pinched TS type of phase diagram can be fully appreciated. The best estimates for the critical point are $T_c = 0.0744$ and $\rho_c = 0.121$. The small value of ρ_c is characteristic of small valence systems [10].

TABLE I. Values of the excess chemical potential μ_{ex}, of the two coexisting densities ρ_{low} and ρ_{high}, and of the simulated box size L. Successive umbrella sampling calculations have been performed with $\Delta N = 5$.

T	μ_{ex}	ρ_{low}	ρ_{high}	L
0.0738	−0.4221	0.059	0.175	18
0.0730	−0.4266	0.048	0.187	14
0.0700	−0.4443	0.025	0.210	14
0.0650	−0.4755	0.0091	0.214	14
0.0600	−0.5086	0.0038	0.202	14
0.0550	−0.5436	0.0019	0.175	14
0.0500	−0.5805	0.0012	0.137	14
0.0450	−0.6190	0.0006	0.098	18

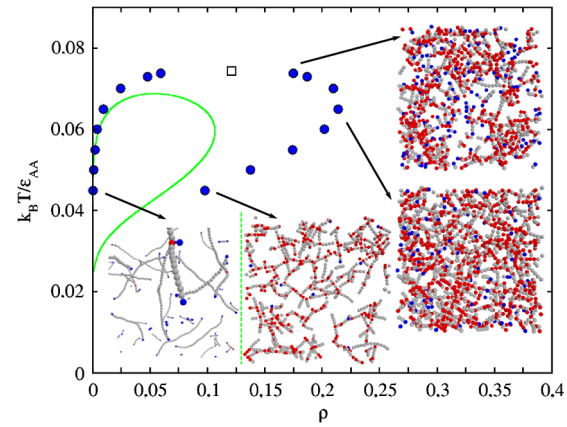

FIG. 3 (color online). Phase diagram of the model in the T-ρ plane. Symbols refer to simulation data, while the line describes the result of Wertheim's theory. Circles are coexistence points, while the open square is the estimated critical point. The pictures show the structure of a slab (of width 5σ for the high-density phase, and L for the low-density phase) of the system for selected points along the numerical coexistence line. The dashed line separates coexisting low and high-density configurations at $T = 0.045$. In the online-color version chain ends are colored blue and junction particles are colored red.

Along with the numerical results, Fig. 3 shows also the theoretical coexistence line predicted with the Wertheim theory. In agreement with previous studies of patchy models, Wertheim theory underestimates the ρ width of the coexistence region (at fixed T), but it gives accurate estimates of the T range where the coexistence is to be expected and, more importantly, it predicts the correct pinched behavior of the phase diagram.

Figure 3 also displays snapshots of the simulated system at different state points along the coexistence line, highlighting the presence of ends and junctions. In the high-density branch, the number of junctions exceeds the number of ends. By lowering T, the number of junctions decreases, leading to a progressive chaining. The visual inspection is quantified in Fig. 4 where the fraction of ends n_e [panel (a)] and junctions n_j [panel (b)] is reported along the numerically determined coexistence line, evaluated both from simulations and Wertheim's theory. Simulations and theoretical results are in good agreement. The figure also shows that the high-density branch is rich in junctions, while the low-density branch is rich in chain ends, in agreement with the TS predictions. Simulations of strongly dipolar fluids [26] also found that, for the same T, higher (lower) densities contain more junctions (ends) than ends (junctions). At the critical point, the number of junctions is larger than the number of ends.

It is important to note that all the ingredients of the pinched phase diagram are well described by the first-order perturbation theory of Wertheim, and indeed the free energy of the TS topological phase transition can be derived as the limit of strong association within the Wertheim theory [12]. This reveals that the mechanism which drives

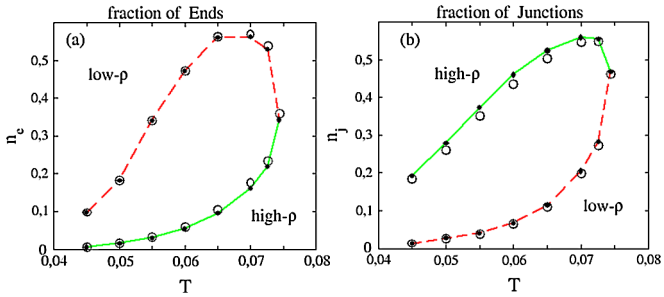

FIG. 4 (color online). T dependence of (a) the fraction of chain ends n_e and (b) the fraction of junctions n_j along the MC coexistence curve for simulations (closed symbols) and theory (open symbols), calculated using the laws of mass action and the simulation data for coexisting densities and temperatures. Note that $n_e = 2X_A$, $n_j = f(1 - X_B)$. The full and dashed lines represent a guide to the eye for the high-ρ branch and the low-ρ branch, respectively.

the phase transition is the condensation of particles in a percolated network, as in the ordinary gas-liquid phase separation, and that the same mechanism can equivalently be described in terms of thermodynamics of the lowest energy chain defects (ends and junctions). Interestingly, both approaches predict a pinched phase diagram only for a limited range of values of the actual energy cost of forming a junction. The present model will thus display (or not) a critical point, depending on the energy scales for chaining and branching, and so is potentially useful for studying systems where phase separation and aggregation compete. This is further facilitated by the availability of a closed-form expression for the free energy from thermodynamic perturbation theory. In addition it might be a first step towards elucidating whether the simplest model dipolar fluid—the dipolar hard-sphere fluid—actually has a critical point, for which there is no conclusive evidence [26,27]. However, true dipolar fluids display additional complications relating to the long range of their interactions, which are poorly understood at present.

Finally, we note that the progressive decrease of the density difference of the coexisting phases may be related to the results of [10], providing an example of temperature controlled effective valence.

J. R. and F. S. acknowledge support from ERC-226207-PATCHYCOLLOIDS and ITN-234810-COMPLOIDS. The other authors acknowledge financial support from the Foundation of the University of Lisbon and FCT under Contracts No. POCI/FIS/55592/2004, No. POCTI/ISFL/2/618, and No. PTDC/FIS/098254/2008.

[1] T. Tlusty and S. A. Safran, Science **290**, 1328 (2000).
[2] P. G. de Gennes and P. A. Pincus, Phys. Kondens. Mater. **11**, 189 (1970).
[3] G. S. Rushbrooke, G. Stell, and Hoye, Mol. Phys. **26**, 1199 (1973).
[4] J. J. Weis and D. Levesque, Phys. Rev. Lett. **71**, 2729 (1993).
[5] R. P. Sear, Phys. Rev. Lett. **76**, 2310 (1996).
[6] R. van Roij, Phys. Rev. Lett. **76**, 3348 (1996).
[7] P. I. C. Teixeira, J. M. Tavares, and M. M. Telo da Gama, J. Phys. Condens. Matter **12**, R411 (2000).
[8] F. Sciortino, A. Giacometti, and G. Pastore, Phys. Rev. Lett. **103**, 237801 (2009).
[9] A. G. Zilman and S. A. Safran, Phys. Rev. E **66**, 051107 (2002).
[10] E. Bianchi, J. Largo, P. Tartaglia, E. Zaccarelli, and F. Sciortino, Phys. Rev. Lett. **97**, 168301 (2006).
[11] J. M. Tavares, P. I. C. Teixeira, and M. M. Telo da Gama, Mol. Phys. **107**, 453 (2009).
[12] J. M. Tavares, P. I. C. Teixeira, and M. M. Telo da Gama, Phys. Rev. E **80**, 021506 (2009).
[13] M. Wertheim, J. Stat. Phys. **35**, 19 (1984); **35**, 35 (1984).
[14] M. Wertheim, J. Stat. Phys. **42**, 459 (1986); **42**, 477 (1986).
[15] J. M. Tavares, P. I. C. Teixeira, M. M. T. da Gama, and F. Sciortino, J. Chem. Phys. **132**, 234502 (2010).
[16] N. Kern and D. Frenkel, J. Chem. Phys. **118**, 9882 (2003).
[17] Two sites of type α and β (with α, $\beta = A$, B), belonging to two different particles i and j, respectively, interact with energy $-\epsilon_{\alpha\beta}$ if the following two conditions are fulfilled: (i) the distance between the particles' centers is smaller than $\sigma + \delta_{\alpha\beta}$; (ii) both angles site$_\alpha$-center$_i$-center$_j$ and site$_\beta$-center$_j$-center$_i$ are smaller than $\theta^{\max}_{\alpha\beta}$. For the present model we use $\delta_{AA} = 0.07$, $\delta_{AB} = 0.545$, $\cos(\theta^{\max}_{AA}) = 0.98$, $\cos(\theta^{\max}_{AB}) = 0.946\,1856$. The resulting persistence length of AA linear chains is $P \approx 54\sigma$, bigger than the average chain length between branching points, so that chains can be effectively considered as linear rods.
[18] E. Bianchi, P. Tartaglia, E. La Nave, and F. Sciortino, J. Phys. Chem. B **111**, 11 765 (2007).
[19] J. Russo, P. Tartaglia, and F. Sciortino, J. Chem. Phys. **131**, 014504 (2009).
[20] In the calculation of $\Delta_{\alpha\beta}$ a quadratic expansion of $g_{\rm HS}(\mathbf{r})$ was shown to reproduce the correct result for the entire density range considered.
[21] P. Virnau and M. Müller, J. Chem. Phys. **120**, 10 925 (2004).
[22] B. J. Schulz, K. Binder, M. Müller, and D. P. Landau, Phys. Rev. E **67**, 067102 (2003).
[23] B. Chen and J. I. Siepmann, J. Phys. Chem. B **105**, 11 275 (2001).
[24] A. M. Ferrenberg and R. H. Swendsen, Phys. Rev. Lett. **63**, 1195 (1989).
[25] N. B. Wilding, J. Phys. Condens. Matter **9**, 585 (1997).
[26] G. Ganzenmuller, G. N. Patey, and P. J. Camp, Mol. Phys. **107**, 403 (2009).
[27] P. J. Camp, J. C. Shelley, and G. N. Patey, Phys. Rev. Lett. **84**, 115 (2000).